# Polaron theory of positronium localization and annihilation in xenon

Jiqiang Chen and Bruce N. Miller
*Department of Physics, Texas Christian University, Fort Worth, Texas 76129*
(Received 5 November 1993; revised manuscript received 22 February 1994)

We investigate the quantum states of a light particle (positronium, or Ps) in a disordered medium (fluid xenon). The Ps atom is modeled as a hard sphere which has thermalized in a Lennard-Jones fluid. The purpose of this paper is threefold: first, to test the efficacy of a recent analytic theory by comparing its predictions with available results of path-integral Monte Carlo (PIMC) simulations; second, to explore the Ps-xenon system over a much wider range of circumstances than is possible with PIMC; third, to report predictions for the lifetime of ortho-Ps and the momentum distribution of para-Ps at high density which should be of interest to condensed-matter experimentalists. In sharp contrast with the case of an electron or positron, the reference-interaction-site-model (RISM)-polaron theory produces Ps-fluid pair-distribution functions in good agreement with the PIMC results. As a result, the pick-off decay rate of ortho-Ps in the transition region between localized and extended states is reproduced successfully. We also find that the variance of the momentum distribution of para-Ps agrees qualitatively with experimental measurements of the angular correlation of the annihilation photons. Compared with the behavior at low density, above the critical density up to about $3\rho_c$ the RISM-polaron theory predicts strong confinement of the localized Ps atom and different distortion of the local fluid density, resulting in the monotonic increase of the decay rate and the momentum variance with mean fluid density. As a consequence, the slope of the decay rate is much greater than the extrapolated low density limit predicted by the older density functional theories. These predictions of RISM-polaron theory for the behavior of positronium in a dense fluid suggest that the traditional picture of self-trapping in a fluid is incomplete and call for more careful experimental investigations to resolve this issue.

## I. INTRODUCTION

Positronium (Ps) is a quasiatom consisting of an electron and a positron which is easily formed when a positron is injected into a fluid. This atom shares many of its characteristics with hydrogen and occurs in two forms: parapositronium (singlet spin state), which decays via a $2\gamma$ process with a natural lifetime of $1.23\times10^{-10}$ sec and orthopositronium (triplet spin), which requires a $3\gamma$ decay process and has the much longer vacuum lifetime of $1.47\times10^{-7}$ sec. In practice, the $o$-Ps annihilates in a very short time via a $2\gamma$ process due to the so-called pick-off process in which the positron bound in $o$-Ps annihilates with an electron associated with an atom of the host material. Measurements of the $o$-Ps pick-off decay rate and the $p$-Ps momentum distribution can provide information about the states of the light particle and its environment. As pointed out by Miller and Fan,[1] the decay rate provides a measure of the local distortion of the fluid produced by the Ps atom, and the momentum distribution provides a measure of the localization of the Ps atom due to the "pressure" exerted by the fluid molecules. Positronium annihilation has a special position in the study of the quantum states of an excess light particle in disordered media such as insulating fluids, a subject that has proven to be very useful in condensed-matter physics as it permits the experimental study of the equilibrium states of a self-trapping system.

The density and temperature dependence of the pick-off decay rate have been observed in various simple fluids such as helium, argon, xenon,[2] and molecular fluids such as ethane and methane.[3] Since its de Broglie wavelength is much larger than the mean interatomic distance in a typical fluid, a Ps atom can simultaneously interact with many atoms. Consequently, in certain regions of density and temperature, it creates a region of altered density in which it is localized. The so-called self-trapping phenomenon is most significant near the liquid-vapor critical point where the isothermal compressibility of the fluid is large. The main features of the density dependence of the experimental pick-off decay rate on an isotherm near $T_c$ are (1) at low density, the decay rate increases linearly; (2) the rate of increase soon slows down around the critical point, and (3) following a flat plateau, it increases again. For most fluids, the final upswing at sufficiently high densities has not been investigated.

The momentum distribution of the annihilation products has also been measured in many simple condensed gases for a range of thermodynamic conditions.[4] If the center of mass of the electron-positron pair is at rest, the $2\gamma$ decay process gives off two annihilation photons 180° apart. However, the pair has momentum regardless of whether or not the positronium atom is localized, and therefore there are departures from 180° which are directly proportional to the component of momentum perpendicular to the photon direction. Thus, measurements of the one-dimensional angular correlation (1DAC) of annihilation photons yield the momentum distribution of the annihilating electron-positron pair. It is found in experiments that the self-annihilation of a $p$-Ps atom localized in the host medium contributes a component with a very small full width at half maximum (FWHM) in the

0163-1829/94/49(22)/15615(11)/$06.00  

1DAC spectrum. For helium at $T=1.7$ and 4.2 K, experiments show that the FWHM of the narrow peak, $\theta_{\mathrm{FWHM}}$, increases from 1 mrad ($10^{-3}$ rad) to 2 mrad when the pressure is increased from 1 to 168 atm.[4] For xenon at $T=170$ K, $\theta_{\mathrm{FWHM}}=2.8$ mrad.[5] $\theta_{\mathrm{FWHM}}$ is an important parameter which reflects how strongly the Ps atom is confined in the host medium.

Most existing theories employed for the quantitative description of the self-trapping of a light particle in a fluid, such as density-functional theory (DFT),[2,6] are of the mean-field type. In DFT, a free-energy functional is constructed that depends on both the wave function of the light particle and the local fluid density. Minimizing the free-energy functional with respect to variations in the wave function and the local fluid density results in a pair of coupled equations that can be solved self-consistently. To some extent the DFT approach is successful in describing the self-trapping process of light particles. However, mean-field theory approximations do not account for density fluctuations. DFT predicts that self-trapping occurs only in a specific density interval and that, elsewhere, the localized state collapses abruptly or does not occur. The accompanying discontinuity in annihilation rate is contrary to experiments which show that the transition from extended to localized states and back is smooth.

Reese and Miller recently performed a path-integral Monte Carlo (PIMC) simulation of a Ps atom in xenon at temperatures $T=300$ and 340 K.[7] In order to correctly predict the main features of the experimental measurements of the $p$-Ps pick-off annihilation rate, one of their major goals was to properly account for fluid fluctuations. Their results compare favorably with experiment and offer insights for a better understanding of the behavior and annihilation mechanism of positronium in simple fluids. They considered the Ps atom as a single quantum particle with double the electron mass, a simple model that is often used in the literature[2] and appropriate for this first attempt to study positronium via PIMC. They took a hard sphere as the Ps-Xe interaction and the Lennard-Jones 6-12 potential (with parameters $\sigma=4.0551$ Å, $\varepsilon=229$ K) to model the fluid. PIMC provides a numerically accurate approach for treating this type of system and has been applied to other similar systems consisting of excess electrons[8-10] and positrons[11] in simple fluids. The approach, however, is very cpu intensive, and the convergence is extremely slow at high fluid density. The method can only test a few points, so it is difficult to obtain a good picture of the predictions over the complete range of density and temperature. Reese and Miller carried out their calculations only for densities $\rho^*=\rho\sigma^3=0.017$, 0.088, 0.17, and 0.35.[7] For their hard-sphere excess electron in a hard-sphere fluid, Sprik, Klein, and Chandler's PIMC simulations were carried out only for densities below $\rho^*=0.38$.[8]

Alternatively, the reference-interaction-site-model (RISM)-polaron theory, an analytical theory developed by Chandler, Singh, and Richardson,[12(a)] can be applied over a much broader range. It has yielded qualitatively encouraging results for a number of problems concerning excess electrons and positrons in some disordered systems.[13-17] In this theory, the light particle is represented by the path integral, and therefore quantum fluctuations are naturally included. Although the theory inherits a weak mean-field approximation, the solvent density fluctuations are partially included as well. As a result, it provides a continuous transition from extended to localized states with varying fluid density for the self-trapping process. Very recently we have shown[16,17] that, with the hypernetted-chain closure, the theory can provide a good quantitative description of the particle-fluid pair distribution function $g(r)$ for an excess electron or positron in fluid xenon ($T>T_c$) above the critical density.

The purpose of the present work is to test the RISM-polaron theory against PIMC simulations for the system of a Ps atom thermalized in fluid xenon. To make a direct comparison, we use the same hard-sphere potential $V(r)$ to describe the interaction between the Ps and a xenon atom,

$$V(r)=\begin{cases}\infty, & r\le d\\ 0, & r>d\end{cases}, \tag{1}$$

and the same Lennard-Jones parameters to model the fluid, where $d=2.5$ Å and $d/\sigma\approx 0.62$. The goal of the comparison is to determine if the theory works for positronium annihilation studies, and what results should be expected for this theoretical model of a Ps atom over a larger range of fluid density.

As in the case of a classical fluid, the RISM-polaron theory requires a closure relation that must be determined independently. In contrast with simple fluids, at the present time it is still not clear what kind of closure is appropriate for the RISM-polaron theory and for the specific particle-fluid interaction considered here. To date, several distinct closures have been employed for different systems. Here we test the theory with two of them, Percus-Yevick[18] (PY) and hypernetted-chain (HNC),[19] that are used widely in the modern theory of simple atomic fluids. The comparison provides quantitative criteria for choosing between them and explores the sensitivity of the model to their differences. We find that the PY closure is slightly more successful than HNC for the present system, but it appears that the HNC closure is more generally applicable for a wider variety of potentials. From the results presented in the paper, it will be seen that the RISM-polaron theory underestimates the confinement of the localized positronium at low density, but it yields a good Ps-fluid pair distribution function when compared with the PIMC results. Thus, we are able to reproduce the main features of the experimental pick-off decay rate $\lambda$. In contrast with the existing DFT calculations, in which $\lambda$ and $\theta_{\mathrm{FWHM}}$ never simultaneously agree well with experimental results,[4] the $\theta_{\mathrm{FWHM}}$ obtained from the RISM-polaron theory also qualitatively agrees with experiments.[4] Moreover, well above the critical density, the predicted behavior is significantly different from that described by DFT. For example, we find that both $\lambda$ and $\theta_{\mathrm{FWHM}}$ are monotonically increasing in this region and, moreover, that $\lambda$ increases much faster than the anticipated linear rate predicted by DFT.

It is noted that Sprik *et al.* tried to make a similar

comparison with PIMC simulations for their hard-sphere excess electron in a *hard-sphere fluid*.[8] They compared the (imaginary) time correlation functions and found that the RISM-polaron theory with the PY closure underestimated the confinement of the localized electron. However, for reasons which are unstated, they did not compare the electron-fluid pair distribution function $g(r)$. The issue of closures was not considered either. Consequently, to date, a consensus concerning the suitability of the $g(r)$ predicted by RISM-polaron theory for a light particle with a purely repulsive hard-sphere potential in fluids is lacking. It also needs to be mentioned that the earlier RISM-polaron calculations for a hard-sphere particle were only carried out for a *hard-sphere* fluid, which lacks a critical point.[8,12(b)] Lennard-Jones fluids have proved to be a more realistic model for simple atomic fluids,[19] and were used in later RISM-polaron calculations.[14,20] However, the treatment of the Lennard-Jones fluid in Ref. 14 seems not accurate enough for accounting for the critical behavior. A significant change in the shape of $g(r)$ around the critical point was found by Fan and Miller.[20] There the PY closure was used for the classical Lennard-Jones fluid, although it is more suitable for short-range, repulsive interatomic potentials.[19] In this paper we will use a better description of the classical Lennard-Jones fluid as input for the quantum mechanical computations which we will describe later on, so that we are able to account for the critical behavior more precisely.

The paper is organized as follows: We briefly review the RISM-polaron theory and the closure issue in Sec. II, and describe the computational method in Sec. III. The numerical results are then presented in Sec. IV, and finally the discussion and concluding remarks are given in Sec. V.

## II. RISM-POLARON THEORY AND CLOSURES

We consider a single particle dissolved in a simple fluid in the adiabatic approximation in which the particle is treated quantum mechanically and the xenon atoms classically. From a standard imaginary-time path-integral formulation,[21] the partition function of the system can be written in the following form with boundary condition $\mathbf{r}^1=\mathbf{r}^{p+1}$:

$$Z_p=\lim_{p\to\infty}\prod_{i=1}^{p}\int d\mathbf{r}^i z_0(\mathbf{r}^i,\mathbf{r}^{i+1};\beta/p)\prod_{j=1}^{N}\int d\mathbf{R}^j\exp\{-\beta U(\underline{\mathbf{R}})-(\beta/p)V(\mathbf{r},\underline{\mathbf{R}})\}\ , \tag{2}$$

where $U(\underline{\mathbf{R}})=(\frac{1}{2})\sum u(|\mathbf{R}^i-\mathbf{R}^j|)$ is the solvent interaction potential energy and $V(\mathbf{r},\underline{\mathbf{R}})=\sum v(|\mathbf{r}-\mathbf{R}^j|)$, where $v(|\mathbf{r}-\mathbf{R}^j|)$ is the particle-solvent interaction, and $\underline{\mathbf{R}}$ stands for the set of atomic positions $\{\mathbf{R}^j\}$. In (2), $z_0$ is the free-particle density matrix in the coordinate representation

$$z_0(\mathbf{r},\mathbf{r}';\beta)=[(2\pi)^{1/2}\lambda_{\rm th}]^{-3}\times\exp(-|\mathbf{r}-\mathbf{r}'|^2/2\lambda_{\rm th}^2)\ , \tag{3}$$

where $\lambda_{\rm th}=[\beta\hbar^2/m]^{1/2}$ is the thermal wavelength of the light particle and $m$ is its mass. A simple picture emerging from Eqs. (2) and (3) is that a quantum particle can be represented by a classical ring polymer with $p$ ($p\to\infty$) classical interacting harmonic oscillators (classical isomorphism). In other words, an excess quantum particle which has thermalized in a classical fluid can be described within the context of classical fluid theory.

The reference-interaction-site-model (RISM) was originally introduced by Chandler to study the structure of molecular fluids.[22] Since there is an isomorphism between a quantum particle and the classical ring polymer described above, Chandler, Singh, and Richardson extended the RISM theory by combining the path-integral formulation with Feynman's polaron approximation,[21(b)] and developed the RISM-polaron theory, an analytical representation for a quantum particle-fluid system.[12(a)] The main equation in the theory is

$$\rho h(r)=\int d\mathbf{r}'\int d\mathbf{r}''\omega(|\mathbf{r}-\mathbf{r}'|)c(|\mathbf{r}'-\mathbf{r}''|)\chi(|\mathbf{r}''|) \tag{4}$$

which provides the connection between the particle-fluid direct correlation function $c(r)$ and the particle-fluid pair-correlation function $h(r)$. In Eq. (4), the solvent density-density correlation function $\chi$ [$\chi(|\mathbf{r}-\mathbf{r}'|)=\langle\delta\rho(\mathbf{r})\delta\rho(\mathbf{r}')\rangle$] is an input to the theory and represents the structural influence of the fluid on the state of the light particle. $\omega(r)$ is the zero-frequency component of the polymer probability density function $\omega(r,\tau)$

$$\omega(r)=(\beta\hbar)^{-1}\int_0^{\beta\hbar}d\tau\omega(r,\tau)\ , \tag{5a}$$

where

$$\omega(\mathbf{r},\mathbf{r}';i,j)\equiv\omega(|\mathbf{r}-\mathbf{r}'|;i-j)\to\omega(|\mathbf{r}-\mathbf{r}'|;\tau-\tau')\quad(p\to\infty) \tag{5b}$$

represents the probability density for finding polymer sites $i$ and $j$ near $\mathbf{r}$ and $\mathbf{r}'$, respectively, in the limit of a continuous chain ($p\to\infty$). Within the context of Feynman's polaron approximation,[21(b)] $\omega(r;\tau)$ assumes the following expression in $k$ space:

$$\bar{\omega}(k,\tau)=\exp\left[-k^2\sum_{n\neq0}(1-\cos\Omega_n\tau)/(\beta m\Omega_n^2+\gamma_n)\right]\ , \tag{6a}$$

$$\gamma_n=(6\pi^2\beta\hbar)^{-1}\int_0^{\infty}dk\,k^4\bar{c}^2(k)\bar{\chi}(k)\times\int_0^{\beta\hbar}d\tau(1-\cos\Omega_n\tau)\bar{\omega}(k,\tau)\ , \tag{6b}$$

where $\Omega_n=2\pi n/\beta\hbar$.

Equations (4)–(6) must be solved self-consistently in order to obtain a solution for $\omega(r,\tau)$ and $h(r)$. In so doing, we have to choose a closure relation for $h(r)$ and $g(r)$. In earlier work, the PY closure[18] was employed for a

hard-sphere excess particle,[12(b),14,20]

$$h(r)=-1, \quad r\le d \ , \tag{7a}$$

$$c(r)=0, \quad r>d \ , \tag{7b}$$

while a HNC-like closure[19] was employed for an excess particle with a long-range attractive potential.[13,16,17] The motivation for these choices arose from the analogy with the classical equilibrium theory of fluids and has not yet been justified from a more fundamental argument. In this paper we are going to examine both of these closures with the hope of obtaining some useful information for guiding the further development of a good closure for the RISM-polaron theory. The reduced form of the HNC closure for a hard-sphere potential given in (1) is

$$h(r)=-1, \quad r\le d \tag{8a}$$

$$c(r)=\exp[h(r)-c(r)]-[h(r)-c(r)]-1, \quad r>d \ . \tag{8b}$$

## III. NUMERICAL METHOD

As pointed out by Nichols *et al.*[12(b)] the solution of the RISM-polaron equation for $g(r)$ is a continuous function of $r$ with a discontinuous slope at $r=d$. As a result, $c(r)$ possesses a delta function singularity at $r=d$, i.e.,

$$c(r)=c_\delta\delta(r-d)+f(r) \ , \tag{9}$$

where $c_\delta$ is a constant coefficient and $f(r)$ is continuous everywhere.

In earlier RISM-polaron calculations for a hard-sphere excess particle in a fluid,[12(b),14,20] a variational method was used to determine $c_\delta$ and $f(r)$. The main idea is that the PY closure in Eq. (7) can be expressed as

$$\delta l[c]/\delta c(r)=0, \quad r\le d \ , \tag{10a}$$

$$c(r)=0, \quad r>d \ , \tag{10b}$$

where

$$l[c]=\rho\bar{c}(0)+(16\pi^3)^{-1}\int d\mathbf{k}\bar{c}^2(k)\bar{\chi}(k)\bar{\omega}(k,\tau) \ . \tag{11}$$

The direct correlation function, $c(r)$, can be obtained from Eq. (4) with a good degree of accuracy for given $\bar{\chi}(k)$ and $\bar{\omega}(k,\tau)$ by adjusting a trial function representing $f(r)$ and the parameter $c_\delta$ and checking the constraint (10). According to Eq. (10b), it is easy to find a good trial function for $f(r)$ because $f(r)=c(r)=0$ for $r>0$. For example, Nichols *et al.*[12(b)] took $f(r)$ to be a cubic polynomial for $r\le d$, and the $c_\delta$ and four coefficients in $f(r)$ were then determined by nullifying the variation in $l$. Alternatively, Fan and Miller[20] used a truncated set of spherical Bessel functions with equal success.

However, the variational method for determining $f(r)$ is not applicable if the HNC closure (8) is used. This is simply because the behavior of $f(r)$ for $r>d$ is now unknown. For our purposes we have to employ a more general method that will accommodate both closures.

The approach we will employ is to first determine the $c_\delta$ by variation and $f(r)$ numerically. It has two iteration loops: The first one is the outside loop which is used to evaluate $(\gamma_1,\gamma_2,\ldots,\gamma_n)$. For a given $\bar{\chi}(k)$, we start with an assumed set $(\gamma_1,\gamma_2,\ldots,\gamma_n)$ and obtain the initial $\bar{\omega}(k,\tau)$ from Eqs. (6). Then we run in the second loop to achieve convergent solutions for $h(r)$ and $c(r)$. By using the resulting $h(r)$ and $g(r)$ we obtain a new set of $\gamma$'s and repeat the above procedure until the $\gamma$'s arrive at the required accuracy. The method devised by Fan and Miller[20] was used to speed up the summation in Eq. (6a). The integrals over $\tau$ in Eqs. (5a) and (6b) are carried out by a self-adjusting mesh integration program so that an accuracy of $10^{-5}$ is guaranteed regardless of the shape of the integrands.[20] As for the number of $\gamma$ values selected, we find that there is no significant difference in the final results when we include the first 20 values ($n=20$) or the first 40 values ($n=40$). In fact, for the final runs we selected $n=30$. Fewer than 10 iterations of the entire process yielded at least three-digit accuracy for the $\gamma$'s.

In the second loop, we took $\theta(r)=h(r)-f(r)$ as the iteration variable to obtain convergent solutions for $h(r)$ and $c(r)$. The reason for doing so is that the closure relations in Eqs. (7) and (8) can be simply written in the form $c(r)=F[\theta(r)]$. In particular, $h(r)=-1$ is equivalent to $F[\theta(r)]=-\theta(r)-1$ for $r\le d$. The iteration is carried out via fast Fourier transformation (FFT) techniques on a grid of $N=2^{11}$ points equally spaced with $\Delta r=0.0811$ Å. (Experimentation with finer meshes did not produce noticeable improvements.) This also allows the use of the RISM equation (4) in $k$ space:

$$\begin{aligned}\rho\bar{h}(k)&=\bar{\omega}(k)\bar{c}(k)\bar{\chi}(k)\\&=\bar{\omega}(k)\bar{f}(k)\bar{\chi}(k)\\&\quad+4\pi c_\delta d^2\bar{\omega}(k)\bar{\chi}(k)[\sin(kd)]/kd \ ,\end{aligned} \tag{12}$$

which is simpler in form and easier to use. In Eq. (12) we have used the Fourier transformation of Eq. (9). $c_\delta$ can be calculated from the equation

$$-4\pi c_\delta d^2=\frac{2\pi^2\rho d^2+\int_0^\infty (kd)\sin(kd)\bar{f}(k)\bar{\chi}(k)\bar{\omega}(k,\tau)dk}{\int_0^\infty k\sin^2(kd)\bar{\chi}(k)\bar{\omega}(k,\tau)dk} \ , \tag{13}$$

which results from Eqs. (11) and (10a) because of the equivalence of Eqs. (7a) [or (8a)] and (10a). In each iteration we begin with an initial choice for $\theta(r)$ and substitute it into a closure equation for $f(r)$. With the resulting $f(r)$ or $\bar{f}(k)$ we calculate $c_\delta$ from Eq. (13) and $\bar{h}(k)$ from Eq. (12). After taking the Fourier transform of $\bar{h}(k)$, we complete an iteration and find a new $\theta(r)=h(r)-f(r)$ for the input of the next iteration. To stop the cycle, we require that the error in $h(r)$ for $r\le d$ is less than 0.001 [$h(0)$ should equal $-1$ as the potential (1) is infinite for

$r \leq d$] and that the quantity

$$\Delta\theta = \left| \sum_{i=1}^{N} [\theta^{m+1}(r_i) - \theta^m(r_i)]^2 / N \right|^{1/2} \quad (14)$$

is less than 0.0001. To accelerate convergence the Ng method, in which the $m$th iteration input is obtained from a suitable linear combination of the preceding three iterates, is used.[23] Even so, when approaching the liquid-vapor critical point, between $10^3$ and $10^4$ iterations are required to achieve the stated accuracy in $h(r)$ for a given set of $\gamma$'s.

To accomplish the present study, we need $\chi$ as input; RISM-polaron theory can only be as good as $\chi$. The best possible $\chi$ can, of course, be obtained from Monte Carlo or molecular-dynamics calculations, but this defeats the purpose of constructing a theoretical model. In our previous RISM-polaron studies for a positron and an excess electron in xenon,[16,17] the solutions of the reference-hypernetted-chain (RHNC) equation of simple classical fluids[24] were used. The solutions are found by applying the Rosenfeld-Ashcroft procedure to model the bridge function in the RHNC integral equation with its hard-sphere values, and selecting the sphere diameter which minimizes the free energy of the system. The RHNC equation for simple fluids has also been tested recently by an alternative computational procedure.[25] The results given in Refs. 24 and 25 show that the difference between the solutions of RHNC and the computer simulations is comparable to the uncertainties in the simulation data. For our purposes, we used a computer code designed by Lado[26] to generate the structure factor $S(k)$ of the RHNC solution for xenon with a Lennard-Jones potential ($\sigma = 4.0551$ Å and $\varepsilon = 229$ K) at $T = 340$ and 300 K for various densities to obtain $\bar{\chi}(k) = \rho S(k)$, the Fourier transform of $\chi(r)$. Unfortunately, as pointed out by Lomba,[25] RHNC solutions may not exist in a certain range of fluid density and temperature. For example, we obtained solutions at $T = 340$ K for *all* the desired scaled densities in the range $0 < \rho^* < 0.95$ but found it difficult to obtain solutions at $T = 300$ K (i.e., closer to the critical temperature) when $0.16 < \rho^* < 0.36$. However, we will see that this problem does not greatly affect our conclusions.

## IV. RESULTS

### A. Structural behavior

We first consider the confinement of the positronium, which can be described by the second moment $R^2(t-t') = \langle |\mathbf{r}(t) - \mathbf{r}(t')|^2 \rangle$, the mean-square displacement (MSD) between two polymer particles on the chain separated by an imaginary time displacement $t - t'$ in the interval $[0, \beta\hbar)$. In the RISM-polaron approximation,

$$R^2(t-t') = 6 \sum_{n \neq 0} [1 - \cos\Omega_n(t-t')] / (\beta m \Omega_n^2 + \gamma_n) \, . \quad (15)$$

In Fig. 1, the results of $R(t-t')$ (RMSD) from PIMC and RISM-polaron theory with the PY closure are plotted. If the RMSD takes on values in a narrow range, or if its maximum value at $t - t' = \beta\hbar/2$ is small, then the Ps atom is strongly compressed. To quantitatively understand the dependence of the RMSD on density, the maximum value of the RMSD, $R(\beta\hbar/2)$, as a function of $\rho^*$ is plotted in Fig. 2. It clearly shows that the RISM-polaron theory greatly underestimates the confinement in the low density region. For high density, above $\rho^* = 0.35$, there are no PIMC data available, but the RISM-polaron theory predicts that, up to $\rho^* = 0.95$, the

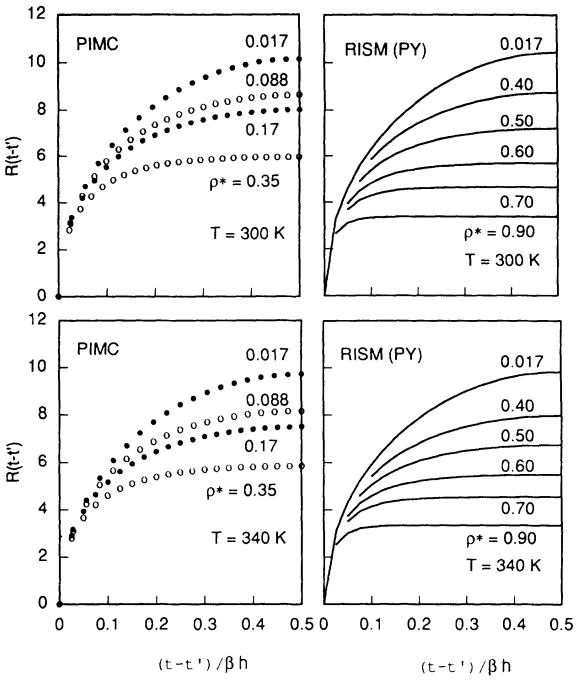


FIG. 1. The comparison of the RMSD between the PIMC simulations (left column) and the RISM-polaron theory predictions with the PY closure (right column) for various fluid densities $\rho^*$ at $T = 300$ K (upper graphs) and 340 K (lower graphs). Because of symmetry, only the data for $0 \leq t - t' \leq \beta\hbar/2$ are plotted.

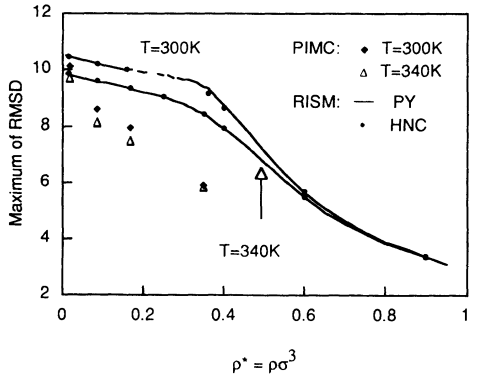


FIG. 2. The maximum value of RMSD [$R(t-t')$ evaluated at $t - t' = \beta\hbar/2$] as a function of fluid density from $\rho^* = 0.0$ to 0.95 for $T = 300$ and 340 K. The available PIMC results are only for $\rho^* = 0.017$, 0.088, 0.17, and 0.35. The dashed line is interpolated in $0.16 < \rho^* < 0.36$ for the RISM-polaron theory with PY closure at $T = 300$ K.

higher the fluid density, the more compressed is the Ps atom. If, as we expect, this is also true for PIMC, the theoretical prediction could "catch up" to that predicted by PIMC at about $\rho^* \approx 0.60$. This contrasts strongly with the comparison by Sprik, Klein, and Chandler,[8] where the two are already almost equal when $\rho^* = 0.373$. There could be many reasons to explain the difference, but we believe that the most important one is that *here* the thermal wavelength is small. Our value of $\lambda_{th}$ is $2.99\sigma$ for $T = 300$ K and $2.81\sigma$ for $T = 340$ K, less than half of that considered in Ref. 8. This suggests that, all things being equal, RISM-polaron theory does better with a longer $\lambda_{th}$. Since a larger $\lambda_{th}$ allows the Ps atom to interact with more fluid atoms, as it does at high density, we also expect that RISM-polaron theory will be more effective at high density. In other words, it is very likely that the $R(t-t')$ resulting from simulations will follow the same trend at high density as that predicted by the RISM-polaron theory and shown in Figs. 1 and 2.

It is seen from Fig. 2 that the RMSD of the RISM-polaron theory begins to change its behavior at $\rho^* \approx 0.33$ for $T = 300$ K and at $\rho^* \approx 0.28$ for $T = 340$ K. This is an indication of the response for the RISM-polaron theory to the critical point of the Lennard-Jones fluid under consideration, for which $\rho_c^* = 0.35$ and $T_c = 289$ K.[7] It shows that, although the size of the response is small, the RISM-polaron theory does reflect the critical region. It is also seen from Fig. 2 that a small discrepancy occurs between the two closures in the critical region (see the curve for $T = 300$ K), in which the HNC closure results in a slightly more compressed Ps atom than that induced by the PY closure. However, in general, there is no *significant* difference between the corresponding theoretical predictions for the compression of the Ps atom.

The Ps atom to solvent radial distribution function $g(r) = h(r) + 1$ is the other central quantity describing localization. It reveals the local fluid distortion produced by the Ps. The available PIMC results are for $\rho^* = 0.017$, 0.088, 0.17, and 0.35 at $T = 340$ and 300 K and we compare them with the RISM-polaron results in Figs. 3 and 4, respectively. The general picture which emerges shows that the two are in good agreement. In particular, the magnitudes of $g(r)$ at short distances, say for $r < 10$ Å, are very close. However, the disagreement at large distance is obvious. The $g(r)$ from PIMC simulations goes to unity from above, which contrasts with the theoretical predictions where it goes to unity from below. We suspect[27] that the disagreement could be a result of the periodic boundary conditions imposed in the PIMC simulations.[7] If this is the case, we would expect better agreement with the $g(r)$ generated by a larger simulation. We do observe a disagreement that appears to be an intrinsic result of the RISM-polaron theory, in which the slope of $g(r)$ at $r = d$ is discontinuous. Also, as numerically indicated in Figs. 3 and 4, $g''(r = d+) < 0$, where $d+$ represents a distance infinitesimally larger than $d$. But what we have seen in the figures is that the PIMC simulations seem to produce a $g(r)$ with a continuous slope at $r = d$ and $g''(r = d+) > 0$.

The general dependence of $g(r)$ on fluid density, as predicted by the polaron theory, is shown in Fig. 5 for

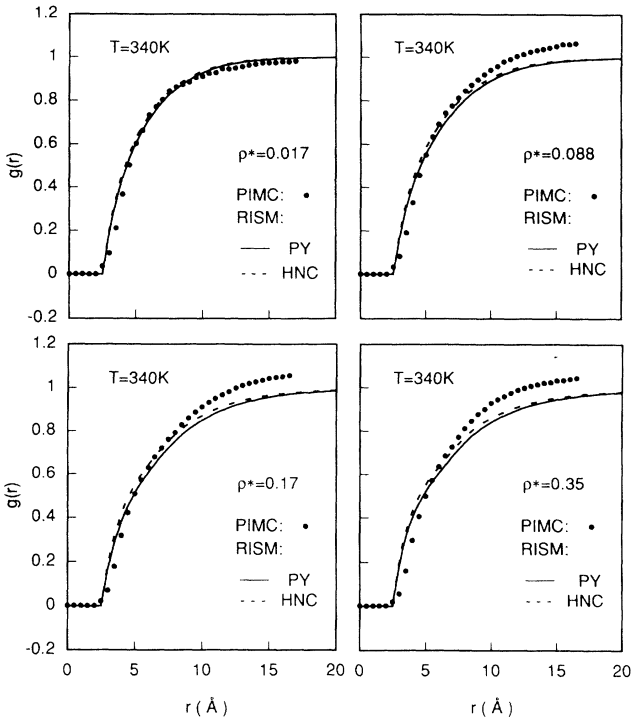


FIG. 3. The comparison of the Ps-xenon radial distribution function $g(r)$ between the PIMC simulations and the RISM-polaron theory predictions for fluid densities $\rho^* = 0.017$, 0.88, 0.17, and 0.35 at $T = 340$ K.

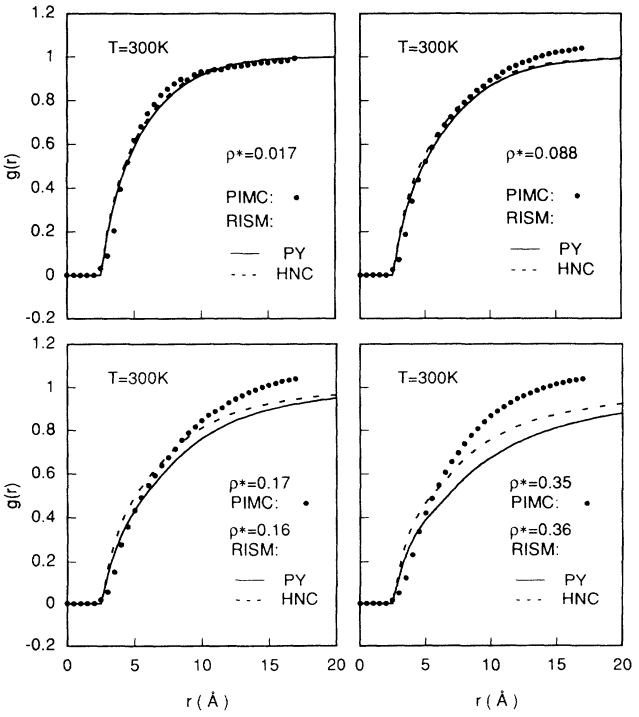


FIG. 4. Comparison of the Ps-xenon radial distribution function $g(r)$ as predicted by PIMC and RISM-polaron theory for various fluid densities at $T = 300$ K. Because of the difficulty in obtaining RHNC solutions for $\rho^* = 0.17$ and 0.35, instead we plot $g(r)$ from the RISM-polaron theory at $\rho^* = 0.16$ and 0.36 in the lower graphs.

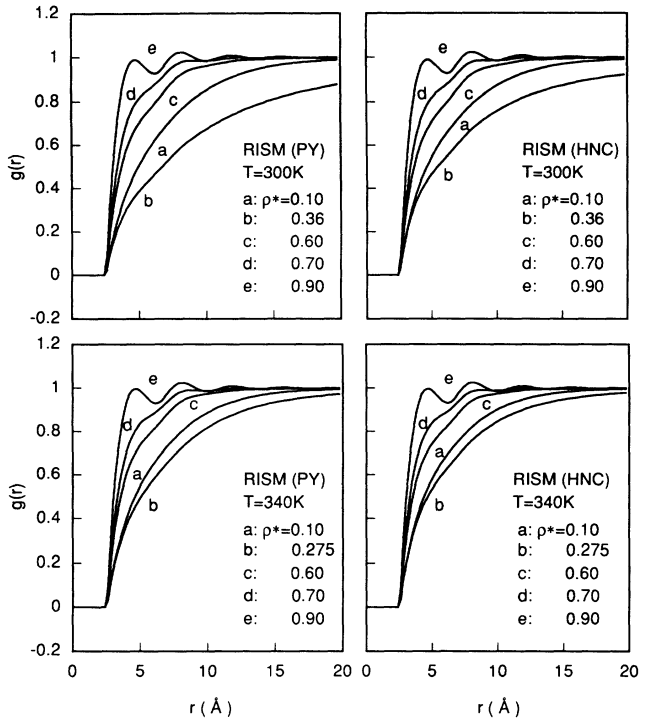


FIG. 5. The Ps-fluid pair distribution function $g(r)$ predicted by RISM-polaron theory with the PY closure (left column) and with the HNC closure (right column) at $T=300$ K (upper graphs) and $T=340$ K (lower graphs) for various fluid densities.

$T=300$ and 340 K. As also illustrated by Nichols *et al.* in Ref. 12(b), we see that the dependence on $\rho^*$ at a given value of $r$ is not monotonic. But what we emphasize here is that, for our present system, the lack of monotonicity corresponds explicitly to the critical behavior of the fluid: at small distances the rate of approach of $g(r)$ to unity becomes minimized when the fluid approaches its critical point. To see this more quantitatively, in Fig. 6 we plot the density dependence of the distance $z$ at which $g(z)=0.70$. The value of $z$ can be considered as a representation of the slope of $g(r)$ at small distances: the greater $z$, the smaller the slope. For $T=300$ K, which is about 10 K above the critical temperature, we see that, as the density increases from zero, $z$ first monotonically increases until $\rho^*\approx 0.33$ and then reverses direction as we continue up to $\rho^*=0.95$ with $z[\rho^*=0.95]<z[\rho^*=0]$. Similar behavior is found for the higher temperature ($T=340$ K), but the reversal occurs at the smaller density of $\rho^*\approx 0.28$, and $z$ traverses a smaller range. It is expected that, for $T=T_c$, the reversal will occur at $\rho^*=\rho_c$. We observe that, for a given density, $z(T=300\text{ K})>z(T=340\text{ K})$, particularly in the region near the critical density, although the two are close at low density and appear to approach the same constant in the high density limit. This is a consequence of the larger isothermal compressibility at $T=300$ K. We also observe that $g(r)$ is a monotonic increasing function of $r$ at low density, but becomes oscillatory at high density. Considering the good agreement with PIMC shown in Figs. 3 and 4, and the fact that the RISM-polaron theory also provides a good description of the particle-fluid pair distribution function for an excess electron[17] in xenon in the high density region, it is reasonable to consider the theoretically predicted $g(r)$ shown in Fig. 5 to be a good supplement to the PIMC calculations.

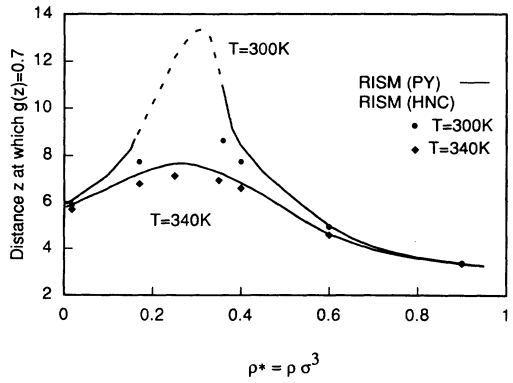


FIG. 6. The plot of the distance $z$ at which the pair-distribution function $g(z)=0.7$ as a function of fluid density $\rho^*$. The results from RISM-polaron theory at $T=300$ and 340 K are presented. The dashed line in the interval $0.16<\rho^*<0.36$ represents the interpolated value from the PY closure at $T=300$ K where the RHNC solutions do not exist.

In the above discussion of $g(r)$, we did not specify which closure was selected. This is because the comparison made in Figs. 3 and 4 shows that each closure considered works well at low density, and Fig. 5 shows that the general picture of $g(r)$ resulting from each is nearly identical. There are some quantitative discrepancies. The $g(r)$ from HNC is generally greater than that obtained from PY for a given $r$, particularly in the critical region (see Figs. 3, 4, and 6). It is interesting to recall that the RMSD generated by the HNC closure is smaller than that resulting from the PY closure in the critical region.

### B. Annihilation properties

The two quantities discussed above, $g(r)$ and $R(t-t')$, characterize the localization of a Ps atom in the fluid. We now discuss their experimental consequences by examining the *o*-Ps pick-off decay rate and the *p*-Ps momentum distribution, which are observables. We discuss the decay rate first.

The pick-off decay rate $\lambda$ of the positron in an *o*-Ps atom annihilating with an electron of a fluid atom can be calculated from the following expression:[1,7]

$$\lambda=(1/8\pi a_0^3)\rho\int d\mathbf{R}\int d\mathbf{r}\exp(-R/a_0)f_{\rm el}(|\mathbf{r}-\mathbf{R}/2|)g(r), \tag{16}$$

where $a_0$ is the Bohr radius and $f_{\rm el}(|\mathbf{r}|)$ is the electron charge distribution at $\mathbf{r}$ associated with an atomic nucleus located at the origin. It is seen that $\lambda$ is directly related to $g(r)$, which reflects the distortion of the fluid around the Ps atom. In order to determine an accurate decay rate it is necessary to have a good representation for $f$. This is not an easy task. In their PIMC studies, Reese and Miller[7] investigated various alternatives and finally calculated the decay rate with a $\delta$-function ap-

proximation. In this approximation, the atomic electron distribution $f(|\mathbf{r}-\mathbf{R}|)$ is simply taken to be $\delta(\mathbf{r}-\mathbf{R})$, and expression (16) then becomes

$$\lambda=(1/\pi a_0^3)\rho\int d\mathbf{r}\exp(-2r/a_0)g(r)\ , \tag{17}$$

which is merely the overlap of the molecular center-of-mass coordinates with the portion of the positron wave function falling outside the hard sphere diameter. Using the $g(r)$ resulting from the RISM-polaron theory, the theoretically predicted decay rate can be worked out from Eq. (17). Since the radius of the hard sphere is $d=2.5$ Å $\approx 5a_0$, the exponential term in (17) decays very rapidly for $r>d$. Therefore the decay rate $\lambda$ reflects the nature of the fluid distortion in a very close vicinity of the hard sphere ($r\approx d$). In Fig. 7, we compare our theoretical results with their PIMC simulation counterparts in the low density region. Following Reese and Miller,[7] we have scaled the fluid density, $\rho\rightarrow\rho/\rho_c$, and the decay rate, $\lambda\rightarrow\alpha\lambda$, where $\alpha$ is a parameter chosen so that at very low density the slope of the decay rate is unity. It is seen that the decay rates predicted from the RISM-polaron theory are in good agreement with the PIMC simulation results. In particular, the PY closure results in a better agreement, which is excellent at $T=300$ K. This is not surprising since it is shown in Figs. 3 and 4 that $g(r)$ from PIMC and the RISM-polaron theory are very close to each other in the vicinity of the Ps atom. The thermal wavelength at $T=300$ K is slightly greater than that at $T=340$ K and our results also show the sensitivity of the RIMS-polaron theory to this difference.

When the fluid density becomes higher, the theoretically predicted decay rate shown in Fig. 7 does not appear

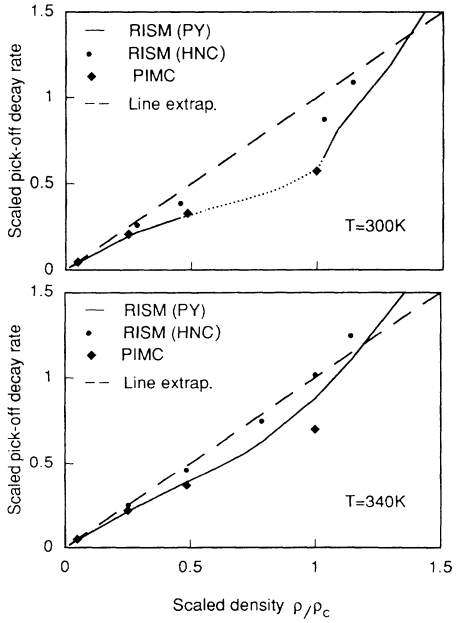


FIG. 7. The scaled $o$-Ps pick-off decay rate (from both PIMC and RISM-polaron theory) as a function of the scaled fluid density $\rho/\rho_c$ at $T=300$ K (upper graph) and $T=340$ K (lower graph) in the low density region. The dashed line in the upper graph is interpolated in the interval $0.16<\rho^*<0.36$ for the RISM-polaron theory with the PY closure.

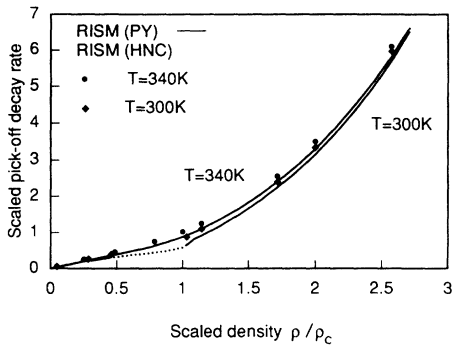


FIG. 8. The scaled $o$-Ps pick-off decay rate predicted from the RISM-polaron theory as a function of the scaled fluid density $\rho/\rho_c$ for values of $\rho/\rho_c$ up to 3 at $T=300$ and 340 K. The dashed line is interpolated in the interval $0.16<\rho^*<0.36$ for the RISM-polaron theory with the PY closure at $T=300$ K.

to be constrained by the long dashed line that is linearly extrapolated from very low density, but rather it increases much more rapidly. To see this more clearly, we plot the decay rate in Fig. 8 for a much larger density region (up to $3\rho_c$). The reason for this unanticipated behavior can be understood from Figs. 5 and 6 which show that the "slope" of $g(r)$ is not constrained by its value at low density when returning from the situation where $g(r)$ has its smallest slope but, rather, the slope continues to increase. Consequently the decay rate does not return to the linear extrapolation at high density.

We now analyze the $p$-Ps momentum distribution $P(\mathbf{p})$. As we mentioned in the Introduction, the experimental $P(\mathbf{p})$ gives rise to a narrow peak in the one-dimensional angular correlation spectrum. The full width at half maximum, $\theta_{\rm FWHM}$, of the narrow peak provides a crude characterization of the $p$-Ps momentum distribution. The variance $q=(\langle p^2\rangle)^{1/2}$ of $P(\mathbf{p})$, or $q_x=(\langle p_x^2\rangle)^{1/2}$ of $P(P_X)$,

$$P(p_x)=\int_{-\infty}^{\infty}dp_y\int_{-\infty}^{\infty}dp_z P(\mathbf{p})\ , \tag{18}$$

is comparable with $(mc)\theta_{\rm FWHM}$ and is readily obtained from the average kinetic energy $E_k=\langle p^2/2m\rangle$: $q=(\langle p^2\rangle)^{1/2}=(2mE_k)^{1/2}$, or $q_x=(\langle p_x^2\rangle)^{1/2}=(2mE_k/3)^{1/2}$. In the RISM-polaron theory $E_k$ can be calculated from the expression[13,14]

$$E_k=-(m/4)[d^2R^2(t)/dt^2]|_{\tau=0}$$
$$=1.5k_BT\left[1+2\sum_{n>0}\gamma_n/(\beta m\Omega_n^2+\gamma_n)\right]\ . \tag{19}$$

The variance $q_x$ resulting from (19) is presented in Fig. 9 as a function of fluid density where $q_x$ has been divided by $mc$ ($c$ is the speed of light) so that the units are radians. It is seen that the variance $q_x$, or $\theta_{\rm FWHM}$, of the 1DAC is directly related to the compression of the Ps atom since it depends solely on $R(t)$. The data at low density shown in Fig. 9 may be questionable because the comparison made in Fig. 1 shows that the theory predicts a less compressed Ps, but the range of magnitude qualita-

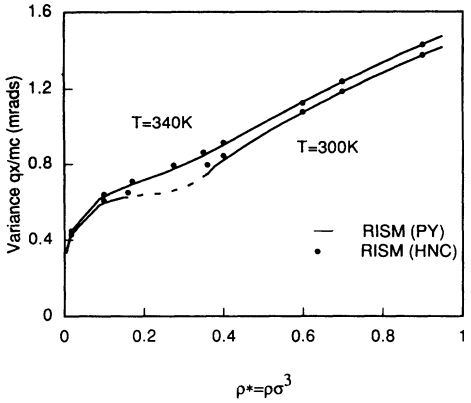


FIG. 9. The variance of the one-dimensional angular correlation distribution of $p$-Ps as a function of fluid density. The results predicted from the RISM-polaron theory at $T=300$ and 340 K are presented. The dashed line is interpolated in the interval $0.16<\rho^*<0.36$ for the RISM-polaron theory with the PY closure at $T=300$ K.

tively agrees with the experimental estimates. For example, for xenon at $T=170$ K, $\theta_{\mathrm{FWHM}}=2.8\ 10^{-3}$ rad.[5] We are not aware of other data available for xenon in this aspect. It is interesting to note that the trend of $q_x$ to high density shown in Fig. 9 is quite similar to that found for helium at $T=1.7$ and 4.2 K where the $\theta_{\mathrm{FWHM}}$ increases with pressure on a given isotherm.[4] We also note that $\theta_{\mathrm{FWHM}}$ at high density is about three to four times greater than that of an extended Ps atom computed from the value of $q_x$ at $\rho^*=0$ shown in Fig. 9. This is expected from Figs. 1 and 2 and the uncertainty principle.

## V. DISCUSSION AND CONCLUSIONS

PIMC is a time-consuming method and it is difficult to use it to cover the complete range of the parameters needed for describing systems such as that considered here. However, the results it provides are numerically accurate, and thus are considered as a testing ground for any analytical theory. In this paper we have compared our RISM-polaron calculations for the system of a Ps atom in xenon with the available PIMC simulation results and investigated the system in the high density region, for which there are no available PIMC data, because the convergence of the simulations is extremely slow there with existing algorithms. From the comparison we have the following immediate conclusions: (1) The RISM-polaron theory can predict a good Ps-fluid pair-distribution function $g(r)$ but underestimates the compression of the Ps atom; (2) both closures, PY or HNC, work well with the theory, but PY seems better; (3) the nonlinearity of the $o$-Ps decay rate in the transition region of the fluid is well reproduced by the RISM-polaron theory. The comparison provides some numerical verification for the closures and the theory, and a justification for accepting the theoretically predicted results extended over a broad range of parameters.

It is seen[29] that the closure problem for the RISM-polaron theory for a light particle with a hard-sphere interaction is not as sensitive as in the case of a particle with a long-range attractive potential tail, such as a positron[16] or an excess electron[17] in xenon. For the latter systems, the HNC closure produces reasonably good results when compared with simulations, but we found difficulties with the PY closure. Due to numerical overflow, the direct application of the PY closure did not converge, while Alnatt's modified version of the closure,[28] although it converges, cannot reproduce the clustering shown in the particle-fluid pair distribution function. In our present system, the PY closure is better than the HNC, but the HNC closure converges and gives reasonable results. Thus, it appears that the HNC closure is more generally useful than PY for the RISM-polaron theory. However, a common weakness of the theory found in the present work and in Refs. 16 and 17 is that the light particles are all predicted to be less localized, particularly in the low density region. It seems that the issue of the closure problem plays a minor role in this respect. Chandler *et al.* attributed this weakness to the polaron approximation which ignores large-amplitude fluctuations,[12(a)] but pointed out that the approximation should be good for high density. The fact that the theoretical results presented in this paper at high density can be considered as a good extension of the PIMC simulations provides convincing evidence for the validity of this conjecture.

From our results we can see that, to some extent, the PY and HNC closures are applicable to the RISM-polaron theory, although these closures are derived from the classical equilibrium theory of simple atomic fluids. This apparent success raises some new questions: First, will different closures which are chosen sensibly strongly affect the results? We have seen that the predictions of both HNC and PY for our system are similar. Second, can a different closure improve the predictions? We have seen that both HNC and PY provide reasonable correlation functions, but underestimate the degree of polymer localization. The lack of chain compression predicted by each closure may be a consequence of the polaron approximation rather than the particular closure. Laria, Wu, and Chandler[15] and Schweizer and Yethiraj[30] have argued that adapting the closures arising in the theory of simple monatomic fluids to a polymer fluid or a polymer in solution may be incorrect. While more work is required to resolve these issues, at least here we have provided both a numerically accurate reference based on the standard closures and direct comparison with PIMC simulations which employ the identical Hamiltonian for a realistic fluid model.

There are two major distinct quantities describing the quantum states of light particles in fluids: the particle-fluid pair-distribution function $g(r)$ and the root-mean-square displacement $R(t)$ (RMSD). The former illustrates the distortion of the fluid produced by the light particle and the latter describes the compression of the particle due to the actions exerted by the fluid atoms. In mean-field theories such as DFT, the stronger the potential well experienced by a particle, the stronger the distortion of the fluid and the compression of the particle. In other words, if the distortion of the fluid is strong, the compression of the particle must also be strong, and vice

versa. A strong potential is produced only in certain ranges of fluid density and temperature and therefore the distortion and the compression do not occur elsewhere. This is not the case in the present calculations where the compression of the Ps atom is a monotonic function of the fluid density in the range concerned, and the distortion of the local fluid occurs in the form

$$g_l = g_0(\text{at } \rho=0) \rightarrow g_l < g_0 \quad (\text{monotonically decreases until } \rho=\rho_m)\,,$$
$$\rightarrow g_l > g_0 \quad (\text{monotonically increases from } \rho=\rho_m)\,,$$

i.e., first increases and then reverses with increasing density, for a given temperature $T$, where $g_l=\rho_l/\rho$ and $g_0=\rho_0/\rho$ [$\rho_l$ represents the value of the local fluid density in the vicinity of the Ps atom and $\rho_0$ its value in the low average fluid density limit ($\rho\rightarrow 0$)]. It appears that if $T > Tc$, then $\rho_m < \rho_c$, and vice versa. Thus, the picture of the localization process which emerges from both PIMC and the RISM-polaron theory is quite different than that of DFT.

Positronium annihilation measurements play a unique role in the study of the localization of quantum particles since, in contrast with the mobility, the two observable quantities, the $o$-Ps pick-off decay rate and the $p$-Ps momentum spread, are equilibrium properties which depend, respectively, on only $g(r)$ or $R(t)$. In DFT, the decay rate at high density approaches the linear extrapolation value since, in that theory, the potential well collapses and $g_l \rightarrow g_0$ rather than $g_l > g_0$. The state of the Ps atom also becomes extended and, therefore, the variance of the $p$-Ps momentum distribution will decrease after achieving a maximum at some density in the range of interest. The substantial differences between our calculations and the predictions of DFT are not surprising, since in the actual fluid the wave function is constrained to move in narrow channels of decreasing width as the density is increased. Therefore, the new predictions deserve experimental exploration. It should be kept in mind that DFT cannot produce a smooth transition region, and cannot simultaneously predict the pick-off decay rate and the variance of momentum distribution with the correct order of magnitude.[4] Our calculations show that the RISM-polaron theory provides a promising tool for studies of positron annihilation and quantum particle localization in fluids.

The $o$-Ps pick-off decay rate is readily obtained from the RISM-polaron theory, as is the variance of the $p$-Ps momentum distribution. However, to obtain the complete momentum distribution function $P(\mathbf{p})$ is not an easy task. Miller and Fan[1] derived $P(\mathbf{p})$ using the path-integral formalism and found

$$P(\mathbf{p}) = (2\pi\hbar)^{-3} \int d\mathbf{r} \exp(i\mathbf{p}\cdot\mathbf{r}/\hbar) \langle \rho_d(\mathbf{r}) \rangle\,, \tag{20}$$

where $\langle \rho_d(\mathbf{r}) \rangle = \langle \rho_d(\mathbf{x},\mathbf{x}') \rangle$ is the density matrix. Since $\mathbf{r}=\mathbf{x}-\mathbf{x}' \neq 0$, the path-integral representation for the Ps atom is not a ring polymer, but rather open ended and separated by $\mathbf{r}$. There is no analytical theory available for quantum particles with the representation of open polymers. A possible approach for computing $P(\mathbf{p})$ is, of course, an extension of the PIMC method, but it appears that large blocks of cpu time will be required. It is fortunate that we can at least obtain the variance of $P(\mathbf{p})$ from the RISM-polaron theory, a ring polymer theory.

Finally we remark that the hard-sphere interaction potential used in the PIMC simulations[7] and the present work is a simplified model for the Ps atom. In fact, the Ps atom is very polarizable with an atomic polarizability eight times greater than that of the hydrogen atom. Obviously the effect of polarization could play an important role in positronium annihilation because it could result in an increase of both the pick-off decay rate and the FWHM of the 1DAC. Since the RISM-polaron theory has demonstrated its ability for describing the hard-core model, it would be interesting to see if it works for a positronium model which includes polarization effects. We are considering this for future work.

## ACKNOWLEDGMENTS

We are grateful to F. Lado for allowing us to use his program to generate RHNC solutions. We also benefited from conversations with T. Reese. The support of the Robert A. Welch Foundation of Houston, Texas through Grant No. P-1002 and the Research Foundation of Texas Christian University is greatly appreciated.

[1] B. N. Miller and Yizhong Fan, Phys. Rev. A **42**, 2228 (1990).

[2] See, for example, M. Tuomissaari, K. Rytsola, and P. Hautojarvi, in *Positron Annihilation Studies of Fluids*, edited by S. Sharma (World Scientific, Singapore, 1988), p. 444, and references therein.

[3] J. D. McNutt and S. C. Sharma, J. Chem. Phys. **68**, 130 (1978).

[4] See, for example, A. T. Stewart, C. V. Briscoe, and J. J. Steinbacher, Can. J. Phys. **68**, 1362 (1990).

[5] S.-T. Wu and G.-S. Yan, J. Chem. Phys. **77**, 5799 (1982).

[6] See, for example, M. J. Stott and E. Zaremba, Phys. Rev. Lett. **38**, 1493 (1977); B. N. Miller and T. L. Reese, Phys. Rev. A **39**, 4735 (1989); T. L. Reese and B. N. Miller, *ibid.* **42**, 6068 (1990).

[7] T. Reese and B. N. Miller, Phys. Rev. E **47**, 2581 (1993).

[8] M. Sprik, M. L. Klein, and D. Chandler, J. Chem. Phys. **83**, 3042 (1985).

[9]D. F. Coker, B. J. Berne, and D. Thirumalai, J. Chem. Phys. **86**, 5689 (1987).

[10]D. F. Coker and B. J. Berne, in *Excess Electrons in Dielectric Media,* edited by C. Ferradini and J.-P. Jay-Gerin (CRC, Boca Raton, 1991).

[11]G. A. Worrell and B. N. Miller, Phys. Rev. A **46**, 3380 (1992).

[12](a) D. Chandler, Y. Singh, and D. M. Richardson, J. Chem. Phys. **81**, 1075 (1984); (b) A. L. Nichols, D. Chandler, Y. Singh, and D. M. Richardson, *ibid.* **81**, 5109 (1984).

[13]G. Malescio and M. Parrinello, Phys. Rev. A **35**, 897 (1987).

[14]D. Laria and D. Chandler, J. Chem. Phys. **87**, 4088 (1987).

[15]D. Laria, D. Wu, and D. Chandler, J. Chem. Phys. **95**, 4444 (1991).

[16]Jiqiang Chen and B. N. Miller, Phys. Rev. E **48**, 3667 (1993).

[17]Jiqiang Chen and B. N. Miller, J. Chem. Phys. **100**, 3013 (1994).

[18]J. K. Percus and G. J. Yevick, Bull. Am. Phys. Soc. **5**, 275 (1960).

[19]See, for example, J. P. Hansen and I. R. McDonald, *Theory of Simple Quids* (Academic, London, 1986).

[20]Y. Fan and B. N. Miller, J. Chem. Phys. **93**, 4322 (1990).

[21](a) R. P. Feynman and A. R. Hibbs, *Quantum Mechanics and Path Integrals* (McGraw-Hill, New York, 1965); (b) R. P. Feynman, *Statistical Mechanics* (Benjamin, Reading, MA, 1972).

[22]D. Chandler, *Studies in Statistical Mechanics VIII,* edited by E. W. Montroll and L. J. Lebowitz (North-Holland, Amsterdam, 1982), p. 275, and references cited therein.

[23]C. Ng, J. Chem. Phys. **61**, 2680 (1974).

[24]F. Lado, S. M. Foiles, and N. W. Ashcroft, Phys. Rev. A **28**, 2374 (1983).

[25]E. Lomba, Mol. Phys. **68**, 87 (1989).

[26]F. Lado (private communication).

[27]The length of the box in the PIMC simulations (Ref. 7) is $3\lambda=9\sigma\approx36$ Å. The periodic condition could result in a peak of $g(r)$ at $r=18$ Å which is the exact position where the $g(r)$ generated from the PIMC simulations gets its maximum, see Figs. 3 and 4.

[28]A. R. Allnatt, Mol. Phys. **8**, 533 (1964).

[29]It is interesting to compare with the result of the paper [Phys. Rev. E **48**, 2898 (1993)] where Chandler studies the Gaussian model of Li and Kardar [Phys. Rev. Lett. **67**, 3275 (1991)], and found that the Percus-Yevick (PY) and mean spherical approximation (MSA) closures have a degree of sensibility for certain classes of interactions between light and fluid atoms.

[30]K. S. Schweizer and A. Yethiraj, J. Chem. Phys. **98**, 9053 (1993).